J.E. Dunn   Roger Fosdick
Marshall Slemrod

Editors

Shock Induced Transitions
and Phase Structures
in General Media

With 85 Illustrations

Springer-Verlag

J.E. Dunn
Sandia National Labs
Numerical Mathematics Division #1534
P.O. Box 5800
Albuquerque, NM 87185 USA

Roger Fosdick
Department of Aerospace Engineering
and Mechanics
University of Minnesota
Minneapolis, MN 55455 USA

Marshall Slemrod
Department of Mathematics
University of Wisconsin
Madison, WI 53706 USA

Series Editors:
Avner Friedman
Willard Miller, Jr.
Institute for Mathematics and its
Applications
University of Minnesota
Minneapolis, MN 55455 USA

Printed on acid-free paper.

NONEQUILIBRIUM MOLECULAR DYNAMICS

WILLIAM G. HOOVER*

Abstract. The development of nonequilibrium molecular dynamics is described, with emphasis on massively-parallel simulations involving the motion of millions, soon to be billions, of atoms. Corresponding continuum simulations are also discussed.

Key words. nonequilibrium, molecular dynamics, massively-parallel, simulation

AMS(MOS) subject classifications. 65C20, 68U20

1. Introduction. I have been working in atomistic computer simulation ever since my graduate-student days with Andy De Rocco at the University of Michigan. My research interests matured in the usual way, shifting from such well-defined equilibrium problems as determining the equation of state, including phase boundaries, to more challenging nonequilibrium problems during the decade from 1960 to 1970. I will describe a few high spots in the development and application of nonequilibrium methods in this talk, emphasizing the recent work that is transforming the field.

Nonequilibrium molecular dynamics[1-3] began around 1970 when Bill Ashurst set out to simulate flows of momentum and energy in nonequilibrium liquids by using boundary heat and momentum reservoirs made up of particles. A typical fluid geometry is illustrated in Figure 1. The methods that Ashurst developed were successfully formalized and generalized about ten years later, in work that is still rapidly developing. He achieved his goal, reproducing the experimental situations leading to nonequilibrium transport. It has turned out that the transport coefficients so determined depend only very slightly on the amount of deviation from equilibrium. Thus the necessarily large gradients in the computer simulations are perfectly acceptable for quantitative work.

By 1980, following pioneering work of Klimenko and Dremin in Russia[4], a joint effort at Los Alamos and Livermore resulted in the simulation and characterization of a strong dense-fluid shockwave[5] using 4800 atoms. The measured structure of that shockwave is compared, in Figure 2, to the predictions of the Navier-Stokes equations, and indicates shear viscosity and heat conductivity coefficients only 30% larger than the small-gradient limits of Newtonian viscosity and Fourier heat conduction. The shockwave transport coefficients are a bit bigger because the relatively rigid and disordered shockwave structure is a more efficient medium for transporting momentum and energy.

Figure 1. "Fluid Walls" used by Ashurst to drive shear flows. Within the walls temperature and mean velocity are controlled by constraint forces. Black disks represent particles moving upward. White disks represent particles moving downward.
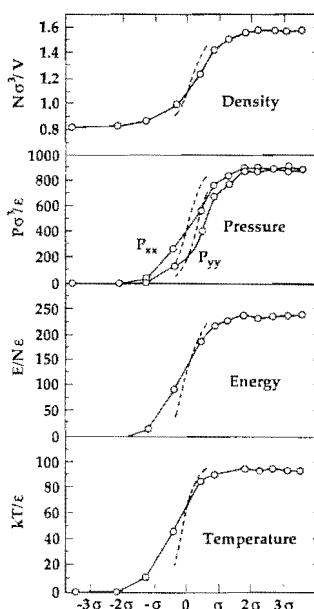
Figure 2. Variation of density, pressure tensor, internal energy, and temperature for a steady strong Lennard-Jones shockwave starting near the triple point. The number density increases from $N\sigma^3/V = 0.844$ to 1.571; the pressure from $P\sigma^3/\varepsilon = 0$ to 917; the internal energy from $E/N\varepsilon = -5$ to 246; and the temperature from $kT/\varepsilon = 0.722$ to 100. The corresponding final temperature for argon is about $12,000$ kelvins, a bit more than one electron volt. The dashed curves were calculated by solving the Navier-Stokes equations, using local values of the transport coefficients. The corresponding results from molecular dynamics are indicated by circles.

e shear flows.
are controlled
ricles moving
downward.

Figure 3. Tony De Groot and the 64-transputer SPRINT, built
as a Ph. D. thesis project in the Department of Applied Science,
University of California at Davis-Livermore. Each processor
has a storage capacity of one million words. The machine ex-
ecutes million-atom molecular dynamics at speeds exceeding
those of typical IBM and CRAY mainframe computers.

ternal energy,
es shockwave
sity increases
n $P\sigma^3/\varepsilon = 0$
246; and the
orresponding
is, a bit more
calculated by
values of the
from molec-

The next advance in simulation was conceptual. By 1985 Farid Abraham and
Carl Moser were vigorously preaching the gospel of fast, cheap parallel computation.
Abraham's simulation of the motion of 161,604 atoms was a breakthrough as signif-
icant as was Rahman's pioneering simulation of many body liquid dynamics with a
continuous force law. Massively-parallel computation became a reality at Livermore
and at Los Alamos a few years later and is now in the process of revolutionizing
computer simulation.

I spent most of the past year in Japan, on sabbatical leave from the University
of California, working in the Physics Department at Keio University in Yokohama,
with my wife, Carol Hoover, on deformation problems involving the motion of up
to one million atoms. The largest simulations were being carried out in Livermore
by Tony De Groot. The goal of simulating the motion of over one million atoms
was articulated and strongly supported by Irv Stowers, leader of the Precision En-
gineering Program at Livermore. The work was made possible by Tony De Groot's
SPRINT[6] computer, shown in Figure 3. At about the same time our calculations
were being developed for the SPRINT, Swope and Andersen[7] were carrying out a
series of million-atom simulated-annealing studies on a large-scale IBM mainframe
computer, the 3090/VF vector processor at Palo Alto.

SPRINT was a pioneering realization of the promise of low-cost parallel compu-
tation. The machine includes 64 transputer processors, cost about $ 40,000 dollars
to build, and can execute a million-atom time step in about thirty seconds. Our
own experience at Livermore, along with similar work at Los Alamos and Palo Alto
shows that transputers, working together, typically match or outperform the main-

frame computers, such as the CRAYs and the IBM 3090/VF, while costing about one thousand times less. The Butterfly at Livermore, with 63 processors, but costing several million dollars, is a few times faster than the SPRINT and mainframe computers. Current chips and the next generation of transputers are both an order of magnitude faster than the transputers in Sprint. Soon teraflop computers will be available.

These computational developments have been paralleled by revolutionary conceptual developments in understanding nonlinear systems and statistical mechanics[2-4,8]. My feeling is that the days of the Langevin equation, much of what is "mathematical physics," and much of what once passed for "applied mathematics," are truly past history. There is now little point in discussing theories which are more complicated than a direct simulation of the phenomena the theories set out to explain. I believe that today's students need to be familiar with simulation in the same way that their grandfathers needed to be familiar with Bessel function expansions, interpolation in seven-place tables of logarithms, and analytic methods for extracting cube roots.

2. Simulations and a Microscopic Second Law of Thermodynamics. Simulations of any system begin with equations of motion. For continua these are Newton's and Fourier's partial differential equations giving the flows of momentum and energy in response to gradients in stress and temperature:

$$\rho \ddot{x} \equiv \nabla \cdot \sigma \equiv -\nabla \cdot P; \rho \dot{e} = \sigma : \dot{\varepsilon} - \nabla \cdot Q;$$
$$\sigma \equiv [-P_{eq}(\rho, e) + \lambda \nabla \cdot u]I + \eta[\nabla u + \nabla u^t]; Q \equiv -\kappa \cdot \nabla T.$$

Here u can represent either the velocity of a Newtonian fluid or the displacement of an elastic Hooke's-Law solid. In the first case λ and η are the fluid's *viscosity coefficients* while in the second case they are the solid's *elastic Lamé constants*. For either fluids or solids P and Q are the *pressure tensor* (minus the stress tensor σ) and the *heat flux vector*; κ is the *thermal conductivity*. The equilibrium pressure P_{eq} as well as λ, η, and κ, *all* depend on the *mass density* ρ and the *energy per unit mass e*.

The atomistic picture *seems* simpler, because it is based on ordinary differential equations of motion rather than partial differential equations:

$$m\ddot{x} = F_{\text{Atomic}} + F_{\text{Boundary}} + F_{\text{Constraint}} + F_{\text{Driving}},$$

but the two approaches, macroscopic and microscopic, are in reality very much alike. Typically the partial differential equations of continuum mechanics are averaged over Lagrangian or Eulerian hydrodynamic zones and the motions of, or within, these zones then satisfy ordinary differential equations. At Livermore Carol, Tony, and I are working on simulations combining the two approaches and suitable for massively-parallel computers using the basic concept exemplified by the SPRINT and Butterfly computers. The continuum studies are being carried out in parallel by our colleagues in Yokohama, Toshio Kawai and Taisuke Boku, both at Keio University.

'F, while costing about
63 processors, but cost-
PRINT and mainframe
uters are both an order
teraflop computers will

d by revolutionary con-
stems and statistical
equation, much of what
for "applied mathemat-
scussing theories which
iomena the theories set
amiliar with simulation
iar with Bessel function
s, and analytic methods

v of **Thermodynam-**
tion. For continua these
ing the flows of momen-
)erature:

Q;

$\equiv -\kappa \ \nabla T$.

uid or the displacement
are the fluid's *viscosity*
tic Lamé constants. For
nus the stress tensor σ)
he equilibrium pressure
and the *energy per unit*

t on ordinary differential
ns:

F_{Driving} ,

1 reality very much alike.
mechanics are averaged
e motions of, or within,
Livermore Carol, Tony,
roaches and suitable for
uplified by the SPRINT
g carried out in parallel
ke Boku, both at Keio

Stable nonequilibrium systems invariably require *thermostats* for the control of temperature. These can best be implemented through a scheme formalized by Nosé, which was a remarkable generalization of Ashurst's approach, and which is precisely consistent with Gibbs' equilibrium statistical mechanics. The "Nosé-Hoover" equations of motion:

$$m\dot{x} = p; \dot{p} = F(x) - \zeta p; \dot{\zeta} = [(K/K_0) - 1]/\tau^2 \Rightarrow \zeta(t) \equiv (1/\tau^2) \int\limits_0^t [(K'/K_0) - 1]dt',$$

use "integral feedback" to force the time-varying kinetic temperature $K(t)$ toward the assigned value K_0 (which is $3NkT_0/2$ for N degrees of freedom in three dimensions) through the friction coefficient ζ. It is remarkable that these equations of motion are *time reversible* [with $-p$ and $-\zeta$ replacing $+p$ and $+\zeta$ in the time-reversed trajectories]. This approach can be generalized. Both space and time dependence can be introduced and several temperatures can be imposed, each with its corresponding friction coefficient. In the general case the rate at which entropy is increased in the external world described by these heat reservoirs is just

$$dS/dt = \Sigma(Q_i/T_i) \equiv \Sigma\zeta,$$

where the sums include all thermostatted degrees of freedom.

The simple time-reversible structure of the "Nosé-Hoover" equations leads to an interesting generalization of Liouville's Theorem. The usual version of Liouville's Theorem states that the phase-space flow of probability density $f(q, p, t)$ takes place at constant density so long as the equations of motion are Hamilton's:

$$\{m\dot{q} = p; \dot{p} = F(q, t)\} \Rightarrow \dot{f}_{eq}(q, p, t) \equiv 0.$$

The Nosé-Hoover generalization of Liouville's Theorem to thermostatted nonequilibrium flows states instead that $f_{neq}(q, p, t)$ *must* **increase** in any nonequilibrium steady state or time-periodic state: $\dot{f}_{neq} \geq 0$. The increase occurs in a topologically interesting way: the probability density seeks out a phase-space strange attractor of reduced dimensionality and diverges on the attractor exponentially fast, as $\exp(\Delta S/k) \equiv \exp(+\Sigma\zeta t) \equiv \exp(-\Sigma\lambda t)$, where the sums include all the friction coefficients and Lyapunov exponents describing the nonequilibrium flow. The alternative to this collapse would be an unacceptable unbounded growth of the occupied region in phase space. Thus the Nosé-Hoover mechanics provides not just a time-reversible analog of thermodynamics consistent with Gibbs' equilibrium statistical mechanics. **It also provides an exact microscopic demonstration of the macroscopic Second Law of Thermodynamics.**

3. Atomistic Simulations and Materials Science. The creative nature of basic research can nurture inefficiency and qualitative, as opposed to quantitative "studies", through a reluctance to interpret and assimilate existing work. By now computer simulation is mature. Qualitative pictures based on incompletely specified

models and untried algorithms are giving way to reproducible *quantitative* studies based on relatively simple models.

In precision engineering there is a need for basic understanding of material failure on a nanometer scale. Because the corresponding physics is nonlinear, and involves many degrees of freedom, theoretical understanding is incomplete. During the last year we developed a simulation of plane-strain indentation, shown in Figure 4, using both a pair potential[9] chosen to match the Lennard-Jones potential for separations less than the inflection point,

$$r < r_i \Rightarrow \phi_{1js} = 4\varepsilon[(\sigma/r)^{12} - (\sigma/r)^6];$$
$$r_i < r < r_m \Rightarrow \phi_{1js} = 3.2920028(\varepsilon/\sigma^3)(r_m - r)^3 - 4.86489008(\varepsilon/\sigma^2)(r_m - r)^2;$$
$$(r_i/\sigma) = (26/7)^{1/6} = 1.24445506; (r_m/\sigma) = 1.737051787,$$

together with a weighted average of this Lennard-Jones-spline potential with an embedded-atom interaction[10-11]. This combination models the greatly-reduced vacancy and defect energy exhibited by typical metals such as copper, silver, and gold:

$$\Phi_{ea} = \Sigma\phi_{ea}(\rho) = (ze\varepsilon/2)\Sigma(\rho_i \ln \rho_i); \rho_i = \Sigma\rho_{ij};$$
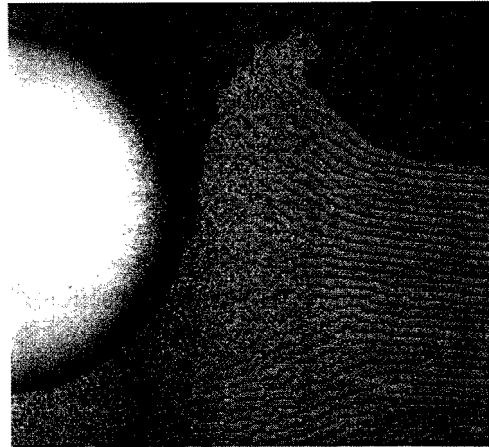$$\rho_{ij} = (1/ze)[(r_m^2 - r^2)/(r_m^2 - d^2)]^2.$$

Figure 4. Portion of a six-day embedded-atom indentation simulation involving 1,036,800 atoms, carried out on SPRINT at Livermore. Prior to indentation similarly-shaded particles occupied horizontal rows. See Reference 12.

The coordination number, z, is 6 in two dimensions. In both cases, Lennard-Jones-spline and (1/3)Lennard-Jones-spline + (2/3)Embedded-Atom, we found[12] that the energy density required to indent a two-dimensional perfect crystal is about one sixth the shear modulus for a plane-strain indentation with a circular indenter. The simulations showed no significant size dependence for crystals with widths exceeding 100 atomic diameters. These results suggest that million-atom simulations in three dimensions should be faithful reflections of reality. We are in the process of extending these same simulations to amorphous solids, both in two dimensions and in three. Such solids are easy to make, following a suggestion furnished by Brad Holian[11] who has investigated the resulting annealing process at Los Alamos. Just take a mechanically unstable lattice, such as the square lattice in two dimensions, and allow the lattice to relax. Figure 5 shows a typical result for an embedded-atom material relaxed for a few atomic vibration times at half the melting temperature. It was surprising to me that the original orientation of the underlying square lattice is not particularly apparent in the resulting amorphous material.
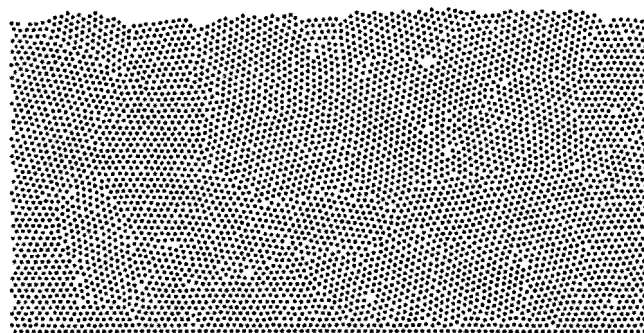

Figure 5. A 5000-atom "amorphous" solid. The forces include both Lennard-Jones-spline pair contributions and embedded-atom many-body contributions. The specimen was annealed from a square lattice at half the melting temperature.

The force history associated with large-scale indentation simulations was likewise unexpected. Typical results are shown in Figure 6. Neither simple static model for constitutive behavior, elasticity or plasticity, predicts such a force-displacement relationship. It may be that *rate-dependent* plasticity is required. Accordingly Carol Hoover, currently at the National Energy Research Supercomputer Center, and I are in the process of developing a simple Lagrangian hydrodynamic program for the SPRINT and Butterfly computers at Livermore. In the time remaining I will describe the model upon which that computer program is based.
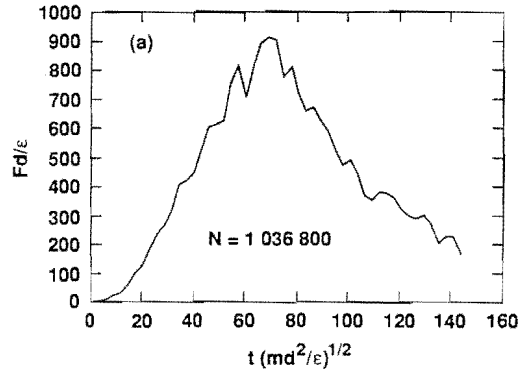
Figure 6. History of the indenter force during indentation of a 1,036,800-atom crystal with an indenter speed equal to a few percent of the sound speed. The force profile corresponds rather closely to indenter velocity rather than to the area of contact between indenter and workpiece. See Reference 12.

4. Continuum Simulations and Materials Science. To keep things simple we represent an elastic-plastic continuum by a set of *triangular* Lagrangian zones. A typical indentation problem is shown in Figure 7. Each zone has associated with it an elastic strain tensor $\{\varepsilon_{xx}, \varepsilon_{xy} \equiv \varepsilon_{yx}, \varepsilon_{yy}\}$ giving the shear deviation of its stress tensor from the equilibrium stress. The velocity field within each zone is assumed to very linearly with x and y, so that, throughout each zone, all three components of the strain rate tensor $\{\dot{\varepsilon}_{xx}, \dot{\varepsilon}_{xy} \equiv \dot{\varepsilon}_{yx}, \dot{\varepsilon}_{yy}\}$ are constant. For simplicity we treat the *shear* deformation according to linear elasticity with a density-dependent *bulk* modulus based on a two-dimensional nearest-neighbor Lennard-Jones potential interaction:

$$\Phi/N = 3\varepsilon[(\rho/\rho_0)^6 - 2(\rho/\rho_0)^3]; P_{eq}V/N = 18\varepsilon[(\rho/\rho_0)^6 - (\rho/\rho_0)^3].$$

In this case the two Lamé constants are equal and are related to the two-dimensional bulk and shear moduli as follows:

$$\lambda \equiv \eta \equiv G \equiv (B_{2D}/2) = \varepsilon(N/V)[63(\rho/\rho_0)^6 - 36(\rho/\rho_0)^3].$$

We add to this elastic basis the concept of plastic yielding, so that the material undergoes *inelastic* "plastic" deformation, relaxing with a characteristic time scale τ, whenever the shear stress exceeds a yield stress $Y \equiv \sigma_{\max}$, or, equivalently, whenever the elastic shear strain exceeds a limiting value $\varepsilon_{\max} \equiv Y/\eta$:

$$\sigma_{\text{shear}} \equiv [\sigma_{xy}^2 + (1/4)(\sigma_{xx} - \sigma_{yy})^2]^{1/2} > Y \Rightarrow d\sigma_{\text{shear}}/dt = [Y - \sigma_{\text{shear}}]/\tau.$$
$$\sigma_{\text{shear}} \equiv \eta\varepsilon_{\text{shear}}; \varepsilon_{\text{shear}} \equiv [\varepsilon_{xy}^2 + (\varepsilon_{xx} - \varepsilon_{yy})^2]^{1/2};$$
$$\varepsilon_{xx} \equiv (\partial u_x/\partial x); \varepsilon_{xy} \equiv (\partial u_x/\partial y) + (\partial u_y/\partial x); \varepsilon_{yy} \equiv (\partial u_y/\partial y).$$

In these elastic equations u is the *displacement* vector, *not* a velocity.
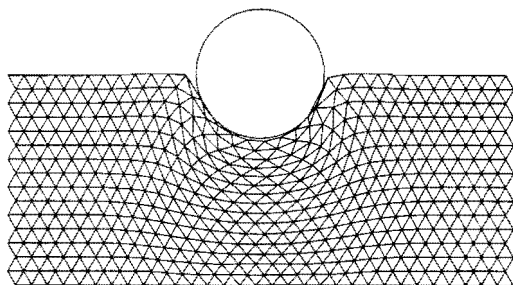
Figure 7. Lagrangian mesh for an elastic-plastic continuum using constant-stress triangular zones. Indentation proceeds by solving discretized differential equations of motion, with rate-dependent plastic stress relaxation.

The combinations of stress and strain components just given are uniquely independent of the orientation of the x and y axes. To make the stress relation likewise independent of orientation requires the six relaxation relations:

$$d\sigma_{xx}/dt = (1/2)(\sigma_{xx} - \sigma_{yy})[Y - \sigma_{\text{shear}}]/(\tau\sigma_{\text{shear}});$$
$$d\varepsilon_{xx}/dt = (1/2)(\varepsilon_{xx} - \varepsilon_{yy})[\varepsilon_{\max} - \varepsilon_{\text{shear}}]/(\tau\varepsilon_{\text{shear}});$$
$$d\sigma_{xy}/dt = (\sigma_{xy})[Y - \sigma_{\text{shear}}]/(\tau\sigma_{\text{shear}});$$
$$d\varepsilon_{xy}/dt = (\varepsilon_{xy})[\varepsilon_{\max} - \varepsilon_{\text{shear}}]/(\tau\varepsilon_{\text{shear}});$$
$$d\sigma_{yy}/dt = (1/2)(\sigma_{yy} - \sigma_{xx})[Y - \sigma_{\text{shear}}]/(\tau\sigma_{\text{shear}});$$
$$d\varepsilon_{yy}/dt = (1/2)(\varepsilon_{yy} - \varepsilon_{xx})[\varepsilon_{\max} - \varepsilon_{\text{shear}}]/(\tau\varepsilon_{\text{shear}}).$$

In each case these contributions to the stress and strain rates are added to the usual convective contributions. The full calculation proceeds by computing $\{\dot{r}, \ddot{r}, \dot{\varepsilon}, \ddot{\varepsilon}\}$ from $\{r, \dot{r}, \varepsilon, \dot{\varepsilon}\}$ by following these steps:

1. Fix initial conditions, specifying $r, \dot{r}, \varepsilon$, and $\dot{\varepsilon}$, and boundary conditions.
2. Compute new coordinates r from nodal and boundary velocities $\dot{r}$.
3. Compute new elastic zone strains ε, and stresses σ, from the strain rate $\dot{\varepsilon}$.
4. Calculate the nodal accelerations $\ddot{r}$ from neighboring zone stresses.
5. Compute zone strain rates taking plastic strain relaxation into account.
6. Return to step 2 until the simulation is complete.

In our implementation it is convenient to solve the differential equations for $r, \dot{r}, \varepsilon$ and $\dot{\varepsilon}$ by using classic fourth-order Runge-Kutta integration. The calculation is about four times more time-consuming than the corresponding atomistic simulation.

The continuum simulation of plastic flow requires relatively "flexible" zoning. When my first efforts, using triangular zones, showed surprisingly little plastic deformation I began to question some of the many experts in continuum plasticity at the Livermore Laboratory. John Hallquist recommended a look at Reference 13, which suggests that straightforward triangular elements cannot describe most plastic flows. Nagtegaal, Parks, and Rice emphasize that a *special arrangement*

of triangular elements *is* sufficiently flexible. See Figure 8. With the help of Jerry Goudreau and Jeff Swegle we are in the process of comparing our molecular dynamics results with both quasistatic and fully dynamic continuum simulations, using a variety of zonings. I hope that these studies will enhance the efficiency of our future goal, fully three-dimensional simulations combining the atomistic and continuum approaches.
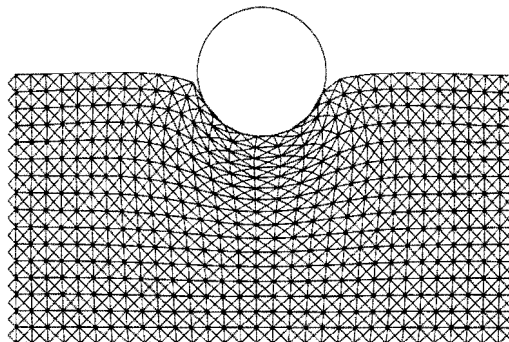

Figure 8. A quadrilateral arrangement of sets of triangular constant stress Lagrangian zones for which the number of degrees of freedom exceeds the number of constraints, as is discussed in Reference 13.
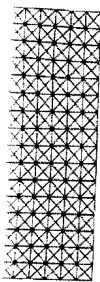
5. Summary. The ideas I have talked about today are not all new. The physical principles go back to Newton and Gauss. The computational ideas are more recent, but can still be traced back to von Neumann. On the other hand the finding that phase-space distributions are *multifractal*, leading to a microscopic proof of the macroscopic Second Law of Thermodynamics *is* relatively new[8,14]. Likewise, the insights that we are finding in our massively-parallel exploration of plastic material behavior in deformation are new, and will likely have a revolutionary impact on materials science.

8. With the help of Jerry
 ...ring our molecular dynam-
 ...nuum simulations, using a
 the efficiency of our future
 ... atomistic and continuum

 ...f triangular con-
 ...mber of degrees
 ... as is discussed

 ...day ...not all new. The
 ...mpu...ional ideas are more
 ... the other hand the finding
 ... a microscopic proof of the
 ...ely new[8,14]. Likewise, the
 ...loration of plastic material
 ...a revolutionary impact on

 ...itute for Mathematics and
 ... work carried out at Keio
 ...een impossible without the
 ...niversity. Carol Hoover, at
 ...ll aspects of the Computer
 ...s, have kindly contributed
 ...equilibrium systems. The
 ...insights of Bill Moran, at

REFERENCES

[1] W.G. HOOVER AND W.T. ASHURST, *Advances in Theoretical Chemistry*, **1** (1975), pp. 1–51.

[2] D.J. EVANS AND G.P. MORRISS, *Nonequilibrium Liquids*, (Academic, New York, 1990).

[3] W.G. HOOVER, *Computational Statistical Mechanics*, (Elsevier, Amsterdam, 1991).

[4] For references and related calculations see W.G. HOOVER, A.J.C. LADD, AND B. MORAN, *High-Strain-Rate Plastic Flow Studied via Nonequilibrium Molecular Dynamics*. Physical Review Letters **48** (1982), pp. 1818–1820.

[5] B.L. HOLIAN, W.G. HOOVER, B. MORAN, AND G.K. STRAUB, *Shockwave Structure via Nonequilibrium Molecular Dynamics and Navier-Stokes Continuum Mechanics*, Physical Review A **22** (1980), pp. 2798–2808.

[6] The SPRINT computer is described by A.J. DE GROOT, S.R. PARKER, AND E.M. JOHANSSON, in *SVD and Signal Processing; Algorithms, Applications and Architectures*, E.F. Deprettere, Editor (North-Holland, Amsterdam, 1988).

[7] W.C. SWOPE AND H.C. ANDERSEN, *Million-Particle Molecular-Dynamics Study of Homogeneous Nucleation of Crystals in a Supercooled Atomic Liquid*, Physical Review B **41** (1990), pp. 7042–7054.

[8] W.G. HOOVER, H.A. POSCH, B.L. HOLIAN, M.J. GILLAN, M. MARESCHAL, AND C. MASSOBRIO, *Dissipative Irreversibility from Nosé's Reversible Mechanics*, Molecular Simulation **1** (1987), pp. 79–86.

[9] B.L. HOLIAN AND D.J. EVANS, *Shear Viscosities away from the Melting Line: Comparison of Equilibrium and Nonequilibrium Molecular Dynamics*, Journal of Chemical Physics **78** (1983), pp. 5147–5150.

[10] The embedded-atom concept was originated by three Sandia scientists, Murray Daw, Mike Baskes, and Steve Foiles. See S.M. FOILES, M.I. BASKES, AND M.S. DAW, *Embedded Atom-Method Functions for the Face-Centered-Cubic Metals, Cu, Ag, Au, Ni, Pd. Pt, and Their Alloys*, Physical Review B**33** (1986), pp. 7982–7991.

[11] B.L. HOLIAN, A.F. VOTER, N.J. WAGNER, R.J. RAVELO, S.-P. CHEN, W.G. HOOVER, C.G. HOOVER, J.E. HAMMERBERG, AND T.D. DONTJE, *Effects of Pairwise versus Many-Body Forces on Plastic Flow*, Physical Review A **43** (1990), pp. 2655–2661.

[12] W.G. HOOVER, A.J. DE GROOT. C.G. HOOVER, I.F. STOWERS, T. KAWAI, B.L. HOLIAN, T. BOKU, S. IHARA, AND J. BELAK, *Large-Scale Elastic-Plastic Indentation Simulations via Nonequilibrium Molecular Dynamics*, Physical Review A **42** (1990), pp. 5844–5853.

[13] J.G. NAGTEGAAL, D.M. PARKS, AND J.R. RICE, *On Numerically Accurate Finite-Element Solutions in the Fully Plastic Range*, Computer Methods in Applied Mechanics and Engineering **4** (1974), pp. 153–177.

[14] H.A. POSCH, W.G. HOOVER, AND B. L. HOLIAN, *Time-Reversible Molecular Motion and Macroscopic Irreversibility*, Berichte der Bunsen-Gesellschaft fuer Physikalische Chemie **94** (1990), pp. 250–256.